

GEOLOGY

Metalliferous Sediments of the Triassic Cherty Formation in the Ol'ga Ore District of Primorye: Tin–Noble Metal Ores of a New Genetic Type

V. T. Kazachenko, E. V. Perevzovnikova, N. V. Miroshnichenko,
A. A. Karabtsov, and V. A. Solyanik

Presented by Academician D.V. Rundqvist November 14, 2005

Received November 14, 2005

DOI: 10.1134/S1028334X0606002X

The Triassic cherty formation of Sikhote Alin [1] hosts metalliferous deposits. They are commonly represented by siliceous–rhodochrosite rocks and their metamorphosed analogues (primarily, consisting of Mn-silicates and aluminosilicates) with high concentrations of Ga, Au, Pt, Pd, and other metals [3]. In the Ol'ga district, the metalliferous deposits are also represented by chocolate-brown siliceous rocks (hereafter, brown cherts) and tin–iron ores.

The metalliferous deposits occur in the Middle–Late Triassic siliceous–clayey sequence. They make up at least one ore-bearing unit (thickness of 5 m or more) represented by brown cherts with a manganese rock bed near the upper contact. The overlying tin–iron ore bed varies from tens of centimeters to a few meters in thickness. Judging from locations of native exposures, talus, and alluvial fragments, the ore-bearing unit is developed over an area of no less than 20 km² (Fig. 1).

The manganese rocks are composed of rhodonite, pyroxmangite, and spessartine with a maximum V₂O₃ content of 0.20 wt % [2, 4]. The rocks contain kanoite, tephroite, manganactinolite, dannemorite, tirodite, pyrosmalite, pyrophanite, hubnerite, scheelite, native silver, native gold, minerals of the cobaltite–gersdorffite series, pentlandite, millerite, violarite, tetradymite, tellurobismuthite, and other minerals. The manganese rocks also include Au (up to 35 g/t), Pt (0.08–0.33 g/t), Zn (up to 5.97 wt %), Cu (up to 0.64 wt %), Ni (up to 0.14 wt %), and Co (up to 0.10 wt %) [3]. Nearly all polished samples contain native silver dissemination up to 20 μm in diameter. Gold grains (*n* mm in size) extracted by the acid treatment of manganese

rocks are characterized by a high grade of fineness (generally, 790) [3].

Tin–iron ores occur as fine-crystalline bedded aggregates represented by talc–chlorite–magnetite and amphibole (manganactinolite)–magnetite varieties. The talc–chlorite–magnetite ore contains ilmenite, sphene, cassiterite, spessartine, sphalerite, quartz, xenotime, and apatite. The ore also includes a Sn-bearing silicate of the following composition (wt %): SnO₂ 3.22–3.82, SiO₂ 23.40, Al₂O₃ 6.23, TiO₂ 24.57, FeO 15.65, MgO 10.54, CaO 1.13, and K₂O 0.07. Based on

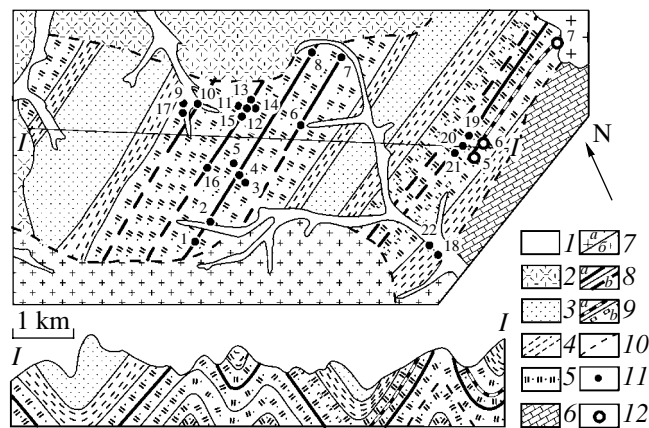


Fig. 1. Schematic geological structure of the Shirokaya Pad area [2, 4]. (1) Quaternary sediments; (2) volcanics of the East Sikhote Alin volcanic belt; (3) sandy sequence (probably, Early Cretaceous); (4) clays and siltstones with tuffite, siliceous rock, and sandstone units (Middle–Upper Jurassic); (5) siliceous–clayey sequence (Middle–Late Triassic); (6) Carboniferous–Permian rocks; (7) granites of the (a) Vladimir and (b) Shirokaya Pad massifs; (8) ore-bearing unit: (a) proved, (b) inferred; (9) unit of Mn- and Fe-rich calcareous–silicate rocks: (a) proved, (b) inferred; (10) fractures; (11, 12) proved exposures: (11) ore-bearing unit, (12) Mn-rich calcareous–siliceous rocks.

Table 1. Compositions of minerals of tin–iron ores (sample Sh-86-43), wt %

Analysis point no.	SiO ₂	CaO	MgO	MnO	FeO	Fe ₂ O ₃	Rh	Ag	Au	SnO ₂	Total
1					2.07	4.13		1.79	92.37		100.36
3	0.73				29.4	66.52					97.15
4			0.51		1.10	2.44	0.92	94.12			98.86
5					1.80	4.00		94.78			100.19
6	1.82	0.97		0.48	7.20					92.19	102.66
17					16.09	35.76				42.73	96.03
18					6.28	13.95				75.76	97.52
19					14.01	31.14				1.37	103.96

Note: (1) Gold (Ag_{0.03}Au_{0.97}) and magnetite; (3) magnetite–gold intergrowth (including 0.43 wt % CoO); (4, 5) silver and magnetite; (6) cassiterite and manganactinolite; (17, 18) cassiterite and magnetite (additional components, wt %: TiO₂ 1.45 in analysis 17; TiO₂ 0.23 and Cr₂O₃ 1.30 in analysis 18); (19) native lead (Sn_{0.04}Pb_{0.96}) and magnetite (additional components, wt %: Cr₂O₃ 0.48 and Pb 56.96). Analyses were carried out on a JXA 8100 microprobe equipped with three wave spectrometers and INCAX-sight energy-dispersive spectrometer in the laboratory of X-ray methods at the Far East Geological Institute, Vladivostok (A.A. Karabtsov, analyst).

Table 2. Chemical compositions of minerals in brown cherts (sample Sh-86-61) underlying manganese ores, wt %

Analysis point no.	Al ₂ O ₃	SiO ₂	TiO ₂	K ₂ O	CaO	Cr ₂ O ₃	MnO	FeO	As ₂ S ₃	BaO	Total
1	20.12	35.64	0.38		1.50		30.51	9.66			98.51
7		0.88	52.86				22.88	19.08			95.70
9		0.51	52.21				21.10	23.04			96.86
11	2.85	39.50		0.94				1.45			101.35
12	4.86	39.39		2.34		1.01	11.66	7.80			82.54**
19	13.98	19.45		1.99	2.32	2.40	1.39	18.73	14.39	3.77	80.22
20	8.65	11.55		0.82	1.48	3.05	0.89	19.30	11.99	5.31	63.04
14	11.51	29.76	0.67	4.55		0.88	0.74	11.80			86.69
16c	4.65	1.26		0.61				19.67	34.19*	5.60	81.72
21	10.05	40.58		4.18			0.93	10.73			95.06

Note: (1) Garnet; (7, 9) pyrophanite; (11) zircon (additional components, wt %: ZrO₂ 56.06 and HfO₂ 0.45); (12, 19, 20) mica-type mineral (additional components, wt %: MgO 1.94, Cl 0.39, Cu₂O 1.54, and PbO 11.81 in analysis 12; Ce₂O₃ 1.80 in analysis 19); (14) mica-type mineral and argentite (additional components, wt %: Mg 4.49, S 3.14, and Ag 19.15); (16c) mica-type mineral and cobaltite (additional components, wt %: S 5.68, Co 10.06); (21) mica-type mineral and silver (additional components, wt %: MgO 4.76, Cl 0.24, and Ag 23.07); (*) As 13.01 and As₂O₃ 21.18; (**) the sum total takes into account the presence of Cl instead of O (2Cl = O).
 Mineral formulas: (12) (K_{0.45}Cu_{0.20}Pb_{0.48})_{1.13}(Mg_{0.44}Mn_{1.50}Fe_{0.99})_{2.93}(Al_{0.87}Cr_{0.12}Si_{5.96})_{6.95}O_k(Cl, OH)_m · nH₂O;
 (19) (K_{0.40}Ca_{0.39}Ba_{0.23})_{1.02}(Mn_{0.18}Fe_{2.44}Al_{0.38})_{3.00}(Al_{2.19}Si_{3.03}As_{1.36}Cr_{0.29}Ce_{0.10})_{6.97}O_k(OH)_m · nH₂O;
 (20) (K_{0.22}Ca_{0.33}Ba_{0.43})_{0.98}(Fe_{2.85}Mn_{0.15})_{3.00}(Fe_{0.50}Al_{2.11}Si_{2.40}Cr_{0.50}As_{1.51})_{7.02}O_k(OH)_m · nH₂O;
 (14) K_{0.95}(Mg_{1.09}Mn_{0.10}Fe_{1.61}Al_{0.20})_{3.00}Al_{2.01}(Si_{4.85}Cr_{0.11}Ti_{0.08})_{5.04}O_k(OH)_m · nH₂O and Ag_{1.93}S_{1.07};
 (16c) (K_{0.22}Ba_{0.62})_{0.84}Fe_{3.00}(Al_{1.54}Fe_{1.63}As_{3.63}Si_{0.36})_{7.16}O_k(OH)_m · nH₂O and Co_{0.98}As_{1.00}S_{1.02};
 (21) K_{0.78}(Mg_{1.03}Mn_{0.11}Fe_{1.38}Al_{0.48})_{3.00}(Al_{1.25}Si_{5.91}Ti_{0.06})_{7.22}O_k(OH)_m · nH₂O and Ag. A.A. Karabtsov, analyst.

the JXA 5A (JEOL) microprobe data, magnetite in this ore includes Zn (0.n wt %), Sn (SnO₂ up to 1.75 wt %), and Ti (TiO₂ up to 1.18 wt %). Talc is enriched in Fe (FeO 1.72–6.63 wt %). Chlorite is represented by the high-Mg and low-Al variety. Cassiterite makes up fine dissemination in magnetite, talc, and chlorite.

The amphibole–magnetite ore contains spessartine, sphalerite, cassiterite, native lead (Table 1), apatite, Pb–Fe phosphate, and a complex sulfide. The Pb–Fe phos-

phate has a variable composition. The first variety Pb_{2.02}Fe_{7.94}[(P_{2.82}Si_{0.26})_{3.08}O_{12.32}](S_{0.98}O_{3.92})(OH)_{8.46} has the following composition (wt %): SiO₂ 0.98, P₂O₅ 12.66, SO₃ 4.97, FeO 36.28, and PbO 28.75. The second variety Pb_{2.00}(Pb_{0.08}Fe_{7.56}Ca_{0.08}Co_{0.01}Cu_{0.17})_{7.90}[(P_{2.90}W_{0.08})_{2.98}O_{11.92}](S_{1.06}O_{4.24})(OH)_{8.66} has the following composition (wt %): P₂O₅ 13.06, SO₃ 5.40, CaO 0.29, FeO 34.53, CoO 0.03, CuO 0.84, WO₂ 1.07, and PbO 29.49. The complex sulfide (Co_{0.10}Cu_{0.23}Ni_{0.64})_{0.97}(Fe_{0.94}Zn_{0.04})_{0.98}(S_{1.95}As_{0.10})_{2.05} has

the following composition (wt %): S 34.14, Fe 28.84, Co 3.23, Ni 20.68, Cu 7.97, Zn 1.31, and As 3.97. Microprobe analyses (Tables 1–3) are often related to the superposition of two or three minerals because of the small dimension of grains. In such cases, the mineral formula is based on the bulk composition. The polished sections nearly always contain fine segregations (up to 20–25 μm in diameter) of Rh-bearing native silver (Table 1). In the elemental spectrum of such segregations, Rh is supplemented with U. According to microprobe data, the U content is rather high (Table 1). In addition, the samples contain native gold grains up to 10–15 μm in size (Fig. 2). Table 1 shows that the gold grains are very pure (finesness up to 981). The tin–iron ores are characterized by high Fe content (FeO as much as 91.37 wt %). Based on the analysis of four samples, the SnO_2 content is 0.65% [4].

The brown cherts are metamorphosed radiolarites with a minor admixture of clayey material. They are composed of quartz, pyrophanite, and a mica-type mineral of the $\text{XY}_3\text{Z}_7\text{O}_k(\text{OH},\text{Cl})_m \cdot n\text{H}_2\text{O}$ composition, where X = K, Ba, Ca, Pb, and Cu; Y = Fe, Mg, Mn, and Al; and Z = Al, As, Cr, Ti, Ce, and Fe (Tables 2, 3). Orthite, monazite, cassiterite, zircon, cobaltite, native iron and silver, and argentite are the subordinate minerals. The

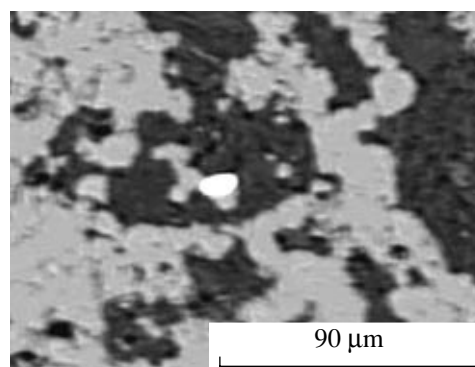


Fig. 2. Native gold in amphibole–magnetite ore (sample Sh-86-43). BSE image showing gold (white), magnetite (light gray), and manganactinolite (dark gray).

cherts also contain spessartine, graphite, rutile, barite, galena, bornite, chalcopyrite, native gold and zinc, phosphide Ni (Ni_5P), halite, sylvite, J- and Br(?)–bearing minerals, Zr–Sc oxide, Zr-bearing rutile, and zinc oxide. The rocks have an augen structure owing to the development of spessartine stringers. The sylvite crystals fill up microscopic cavities in the rock. The halite

Table 3. Chemical compositions of minerals in brown cherts (sample Sh-86-60) overlying tin–iron ores, wt %

Analysis point no.	Al_2O_3	SiO_2	S	K_2O	CaO	Br	MnO	FeO	As_2S_3	Co	Total
5		3.14		0.92		8.02	0.52	23.84	29.39		74.13
7	7.90	32.63	4.77	2.87	0.67		0.67	6.61			89.69
28	2.74	31.41	1.01					3.25			102.75
6	6.97	13.18	1.79				9.51	4.57			93.80
12		26.19	6.59		0.88	14.76	24.33	7.02	13.78*	10.26	105.12
29		14.08	13.00			8.58	7.84	5.94	28.42*	17.71	102.32
25		16.07	9.44	0.27	0.46	10.10	10.69	6.27	24.94*	16.36	98.41
20		23.85	7.18		0.88	12.56	19.16	6.50	15.62*	11.29	97.04
22		1.01	19.13				1.67	4.18	43.48*	26.49	102.71
16		5.24						0.98			98.42
18		31.47						0.58			100.95
32		23.70		28.71**				0.89			89.74

Note: (*) As; (**) K. The sum totals take into account the presence of Br instead of O ($2\text{Br} = \text{O}$). (5) Mica-type mineral (additional components, wt %: ZnO 0.70 and BaO 8.40); (7) argentite and mica-type mineral (additional components, wt %: MgO 2.32 and Ag 31.25); (28) silver, argentite and an unidentified phase (additional components, wt %: MgO 0.81, Cl 0.43, Ag 60.13, and U 2.62); (6) silver, argentite, and garnet (additional components, wt %: MgO 0.61, Ag 54.26, and U 2.91); (12, 29, 25, and 20) cobaltite and an unidentified phase (additional component, wt %: Ni 1.31, 6.75, 3.81, and 0.00, respectively); (22) cobaltite (additional component, wt %: Ni 6.75); (16) cassiterite (additional components, wt %: Na_2O 0.62 and SnO_2 89.54); (18) zircon (additional components, wt %: SrO 2.05, ZrO_2 65.72, and HfO_2 1.21); (32) sylvite (additional components, wt %: P_2O_5 7.24 and Cl 28.33). Mineral formulas: (5) $(\text{K}_{0.28}\text{Zn}_{0.12}\text{Ba}_{0.60})_{1.00}(\text{Mn}_{0.11}\text{Fe}_{2.89})_{3.00}(\text{Fe}_{1.92}\text{As}_{4.31}\text{Si}_{0.76})_{6.99}\text{Br}_{1.44}\text{O}_k(\text{OH})_m \cdot n\text{H}_2\text{O}$; 7 – $\text{Ag}_{1.98}\text{S}_{1.02}$ and $\text{K}_{0.72}(\text{Mg}_{0.68}\text{Mn}_{0.11}\text{Fe}_{1.09}\text{Al}_{1.12})_{3.00}(\text{Al}_{0.78}\text{Si}_{6.41}\text{Cr}_{0.10})_7\text{O}_k(\text{OH})_m \cdot n\text{H}_2\text{O}$; 6 – $(\text{Mg}_{0.21}\text{Fe}_{0.89}\text{Mn}_{1.89})_{2.99}\text{Al}_{1.92}\text{Si}_{3.08}$; (7) $\text{Ag}_{1.98}\text{S}_{1.02}$ and $\text{K}_{0.72}(\text{Mg}_{0.68}\text{Mn}_{0.11}\text{Fe}_{1.09}\text{Al}_{1.12})_{3.00}(\text{Al}_{0.78}\text{Si}_{6.41}\text{Cr}_{0.10})_7\text{O}_k(\text{OH})_m \cdot n\text{H}_2\text{O}$; (6) $(\text{Mg}_{0.21}\text{Fe}_{0.89}\text{Mn}_{1.89})_{2.99}\text{Al}_{1.92}\text{Si}_{3.08}$; (12) $(\text{Co}_{0.89}\text{Ni}_{0.11})_{1.00}(\text{As}_{0.94}\text{S}_{1.05})_{1.99}$ and $(\text{Ca}_{0.29}\text{Fe}_{1.79}\text{Mn}_{4.94})_{7.02}\text{Si}_{7.98}(\text{Br}_{3.38}\text{O}_{21.29})_{24.67}$; (29) $(\text{Co}_{0.75}\text{Ni}_{0.29})_{1.04}\text{As}_{0.95}\text{S}_{1.01}$ and $(\text{Mn}_{3.78}\text{Fe}_{2.84})_{6.62}\text{Si}_{8.36}(\text{Br}_{3.69}\text{O}_{21.50})_{25.18}$; (25) $(\text{Co}_{0.82}\text{Ni}_{0.19})_{1.01}\text{As}_{0.99}\text{S}_{0.81}$ and $(\text{Ca}_{0.24}\text{K}_{0.16}\text{Mn}_{4.35}\text{Fe}_{2.52})_{7.27}\text{Si}_{7.73}(\text{Br}_{3.65}\text{O}_{20.91})_{24.56}$; (20) $\text{Co}_{0.92}\text{As}_{1.00}\text{S}_{1.08}$ and $(\text{Ca}_{0.30}\text{Mn}_{5.23}\text{Fe}_{1.75})_{7.28}\text{Si}_{7.70}(\text{Br}_{3.05}\text{O}_{21.16})_{24.20}$; (22) $(\text{Co}_{0.77}\text{Ni}_{0.20})_{0.97}\text{As}_{1.00}\text{S}_{1.03}$; (32) $\text{K}_{0.96}\text{Cl}_{1.04}$. A.A. Karabtsov, analyst.

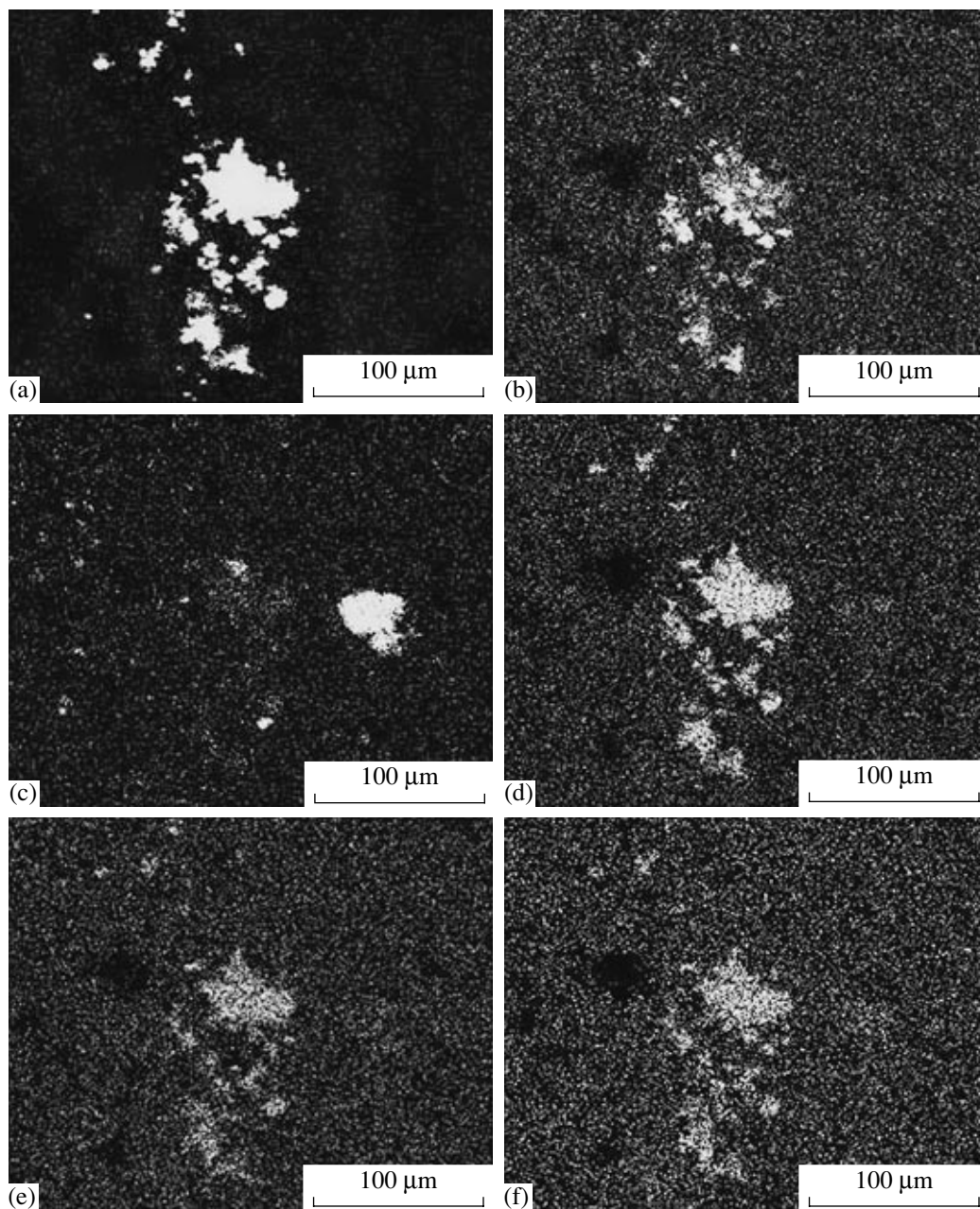


Fig. 3. Characteristic radiation images showing the distribution of (a) Ag, (b) S, (c) Zn, (d) Pd, (e) Rh, (f) Ru, (g) Au, (h) Pt, (i) Ir, and (j) Os in ore minerals and enclosing brown cherts (sample R-80-39). One can see S- and Ag-rich (argentite), Ag-rich and S-poor (native silver), and Zn-rich (zinc oxide) zones. Scale bar 100 μm .

makes up a coating on ore minerals. According to microprobe data (Table 3), the formula of Br(?) -bearing manganese silicate is similar to that of amphibole or pyroxenoid. The presence (or absence) of Br in this mineral remains an open issue.

Based on the microscopic study, all samples of the brown chert contain an abundant dissemination of native silver grains (from 8 to 25 μm in size, up to 60 μm in rare cases) that are usually confined to a mica-type mineral related to metamorphism of the clayey matrix of the rock. Each silver grain is commonly

formed after the radiolarian. The silver grains include dispersed and submicroscopic particles of minerals of Pd, Rh, Ru, Au, Os, Ir, and Pt. Their characteristic radiation images reveal the internal structure of radiolarians in the form of numerous spherical (more intricate in rare cases) segregations. The submicroscopic and dispersed particles of noble metals are present not only in silver grains but also in the whole volume of the enclosing rock. In Fig. 3, the entire surface is covered with a dissemination of submicroscopic particles (bright spots) of minerals of Ag, Pd, Rh, Ru, Au, Pt, Os, and Ir.

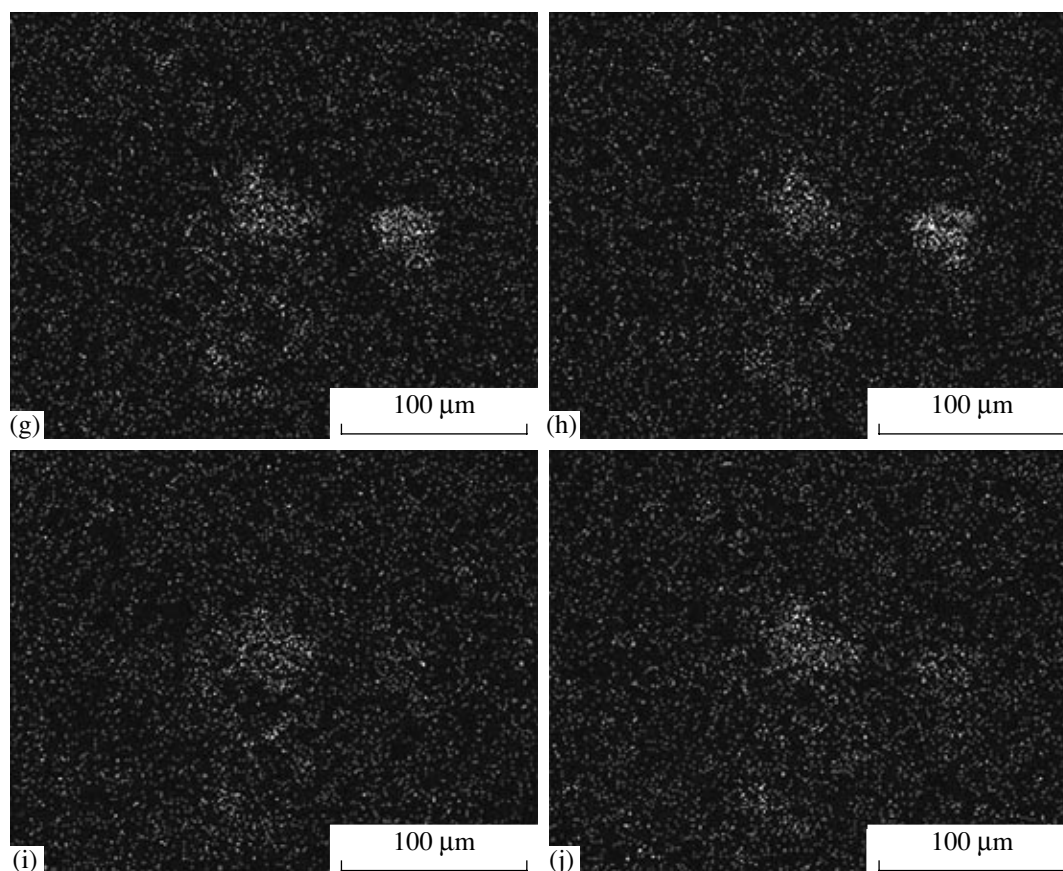


Fig. 3. (Contd.)

Particles of the disperse dimension are abundant in the intergrain space (rings and semirings in the images). The characteristic radiation images often show microfissures filled with relatively large (but rare) gold and platinoid minerals formed after particles of the disperse dimension. In some places, such microfissures crosscut the whole silver grain and enclosing rock.

Elemental spectra of silver grains often (but not always) show the presence of U (in some places, Pu and/or U). Results of microprobe analyses indicate a high U content in these grains (Table 3). Inhomogeneous distribution of silver and uranium in grains is clearly seen in their characteristic radiation images: the darker spots of U radiation correspond to the lighter spots of Ag radiation. The presence of U in the analyses can be related to the superposition of U and Ag lines. However, this issue needs special investigation.

In some places of the brown chert, the largest silver particles make aggregates with argentite and other ore minerals. Pd, Rh, Ru, Pt, Au, Os, and Ir are often differently distributed in ore minerals. For example, Au and Pt are sometimes confined to boundaries of silver and argentite grains or are dispersed in the zinc oxide. Os and Ir, which are virtually absent in the zinc oxide, behave like Au and Pt. Pd, Rh, and Ru are only dis-

persed in the native silver and argentite grains. The Au distribution pattern (Fig. 3) shows that the native silver–argentite aggregate represents two partly replaced radiolarians ~95 μm in size. The zinc oxide fills up the central part of the third radiolarian of a similar dimension. In addition to the brown cherts, numerous fragments of products of their supergene alteration are also present in the study area. Microscopic analyses show that such rocks have the highest concentration of native silver and argentite grains.

The presence of manganese rocks and tin–iron ores can testify to the hydrothermal origin of metalliferous solutions. Noble metals and many other metals were probably absorbed in the ionic state from solutions by the clayey and organic materials of the radiolaria-rich sediment. Their transition to the noble state was promoted by reducing conditions of diagenesis and metamorphism of the brown cherts. The metasomatic formation of microscopic silver particles was related to diagenesis and metamorphism at a relatively low temperature. It is evident that only the above scenario coupled with other favorable conditions could preserve the structural pattern of radiolarians in native silver particles. Results of the preliminary study indicate that the

study region may host a superlarge stratified tin–noble metal deposit of a new genetic type.

ACKNOWLEDGMENTS

This work was supported by the Presidium of the Far East Division of the Russian Academy of Sciences (project no. 05-1-onz-10).

REFERENCES

1. Yu. G. Volokhin, E. V. Mikhailik, and G. I. Buri, *The Triassic Cherty Formation of Sikhote Alin* (Dal'nauka, Vladivostok, 2003) [in Russian].
2. V. T. Kazachenko, *Petrology and Mineralogy of Hydrothermal Manganese Rocks in East Russia* (Dal'nevostochn. Otd. Ross. Akad. Nauk, Vladivostok, 2002) [in Russian].
3. V. T. Kazachenko, N. V. Miroshnichenko, et al., *Gallium, Gold, and Platinoids in Manganese Rocks of the Southern Sikhote Alin Region*, Dokl. Earth Sci. **407**, 429 (2006) [Dokl. Akad. Nauk **407**, 516 (2006)].
4. V. T. Kazachenko and V. I. Sapin, *Mineralogy and Genesis of Ferromanganese Mineralization in the Pribrezhnaya Zone of Primorye* (Dal'nevostochn. Otd. Ross. Akad. Nauk, Vladivostok, 1990) [in Russian].